EARTH SCIENCE FRONTIERS
Volume 16, Issue 6, November 2009
Online English edition of the Chinese language journal

Available online at www.sciencedirect.com
ScienceDirect

Cite this article as: Earth Science Frontiers, 2009, 16(6): 248–256.

RESEARCH PAPER

A Study of Remote Sensing Image Landform Frame and Lithologic Component Decomposing Algorithm and Multifractal Feature of Rock Types

PAN Wei[1,2,*], NI Guoqiang[1], LI Hanbo[2]

1 School of Optoelectronics, Beijing Institute of Technology, Beijing 100081, China

2 National Key Laboratory of Remote Sensing Information and Image Analysis Technology, Beijing Research Institute of Uranium Geology, Beijing 100029, China

Abstract: Landform frame-lithologic component decomposing algorithm for remote sensing (RS) image is proposed according to the principle of optical imaging and fractal feature of landform. The algorithm is applied to decompose the enhanced thematic mapper (ETM) image of rocks for the study of α-$f(\alpha)$ multifractal spectra. The original ETM image, decomposed landform frame and lithologic component subimage are used to calculate the α-$f(\alpha)$ multifractal spectra of adamellite and metamorphic sedimentary rocks in different areas. From the original ETM image, the α-$f(\alpha)$ multifractal spectra do not show any relation to rock types and landform. However, using the decomposed subimage, the adamellite from different areas shows the same α-$f(\alpha)$ spectra feature of the lithologic component subimage, but different α-$f(\alpha)$ spectra features of the landform frame subimage. On the contrary, the adamellite and metamorphic sedimentary rocks in the nearby area have different α-$f(\alpha)$ spectra of the lithologic component subimage, but rather similar α-$f(\alpha)$ spectra of the land frame subimage. This means the land frame-lithologic component algorithm and α-$f(\alpha)$ multifratal spectra can provide a new validated method to improve lithology recognition with RS image texture.

Key Words: remote sensing image; landform frame-lithologic component model; decomposing algorithm; rock types; α-$f(\alpha)$ multifractal spectra

1 Introduction

Lithologic classification and recognition by means of the texture analysis of a remote sensing image has long been a challenge to remote sensing geologists. Different types of texture analysis methods have been developed for image classification. Among them, fractal analysis and wavelet tranform are methods yielding better effects. Fractal is widely used in image classification and object identification. In classifying a remote sensing (RS) image, if fractal dimension is calculated and acted as one of the parameters or eigenvalues, the effects of classifying can be improved greatly[1–4], but the precision is still far behind the visual interpretation. As fractal dimension is regarded as not being able to represent complex fractal objects, multifractal or multifractal spectrum are used a lot more in image texture analysis and object recognition[5,6]. In geoscience, multifractal is often used to study spatial distribution of fractures[7], the singularity of the mineralization process[8], and to emulate the texture pattern of geochemical maps[9]. Wavelet is another widely used method in texture analysis. Due to the multiscale performance, the wavelet can typically be used in the classification and identification of image objects at different levels, and can greatly enhance the precision of image classification and object recognition, by combining with other methods of texture analysis[9–12]. The major problem in decomposing an image with a wavelet is how to determine the decomposition levels. Through reviewing the study results of decomposing algorithm on

Received date: 10-Jun-2009; **Accepted date:** 15-Nov-2009.
* **Corresponding author.** E-mail: panweiprc@yahoo.com.cn
Foundation item: Supported by the Project of National Key Laboratory of Remote Sensing Information and Image Analysis (No. 9140C7201010601) and the Project on Nuclear Energy Development of COSTIND (No. YH061-12).

DOI: 10.1016/S1872-5791(08)60122-0

texture analysis, we found that the most serious problem in texture analysis is to define texture without knowing the genetic mechanism and its physical meaning, and doing it simply from mathematic modeling or statistical understanding. This article tries to find a new method of texture analysis by studying the optical imaging principle of the RS image and the geological meaning of image texture.

2 Surface frame and chemical component model of optical RS image

Due to the optic anisotropy of ground objects, the optical intensity of an object in the remote sensing image is determined not only by object reflectance, but also by object surface structure. Let $f(x, y)$ be the optic image of ground sense composed of different objects in the spatial domain, then $f(x, y)$ can be regarded as the sum of the reflectance of a surface structure with the same reflectance, noted as $g(x, y)$, and the reflectance of the material characterized by the reflectance superimposed to the surface, noted as $s(x, y)$. That is

$$f(x, y) = g(x, y) + s(x, y) \tag{1}$$

In the frequency domain, if the surface structure has a frequency different from the material objects, the image can be decomposed. Because the surface is more smooth and continuous in space than that of the material objects' boundary, so in the wavelet frequency domain it can be represented by the lower frequency part, $W_g(u, v)$, of the decomposed image, and the material objects can be the higher frequency part, $W_s(u, v)$, of the decomposed image. Let $W(u, v)$ be the wavelet transform of $f(x, y)$, then we have

$$W(u, v)=W_g(u, v)\ W_s(u, v) \tag{2}$$

After decomposition, with a reverse transform from frequency to space domain, we can get the decomposed image of $g(x, y)$ and $s(x, y)$ in the spatial domain.

3 Algorithm for decomposing RS image of rocks into landform frame and lithology component

In geology, the texture in a remote sensing image of rocks mainly includes rivers, gullies, fractures and lithological boundaries. To classify rocks with texture, we should first extract the texture closely related to rocks from the image. Although evolution of gullies and rivers is related to lithology, the main controlling factor is the landform frame. As the landform exists with good self-similarity, its spatial frame features can be well presented by fractal dimension[13,14]. Therefore, the fractal dimension of the digital elevation model (DEM) should be equivalent to that of the lower frequency part of the decomposed RS image, provided the landform frame has been subtracted from the image, and the decomposed level by wavelet can be judged by calculating the fractal difference between DEM and the low frequency subimage. The algorithm for decomposition of the RS image into the landform frame and lithologic component subimage can be shown in Fig. 1.

As rocks are anisotropic, high frequency subimages of horizontal, vertical, and diagonal directions should be recorded by wavelet transform in the lithologic component subimages. The development of rock texture must be closely related to the lithology, mode of occurrence, and the stress applied to them. The anisotropy of the three directions results in the anisotropy of the rock texture. Therefore, an analysis of the similarities and differences of lithology must consider the results in the subimages from all the three directions. In this article, image decomposing is done with MATLAB, and the fractal dimension and multifractal spectrum are calculated by the FracLab software.

4 Hölder exponent and multifractal spectrum

There are different methods to describe multifractal spectrum, the most common and accurate ones are the α-$f(\alpha)$ spectrum and the q-D_q spectrum[15]. In texture analysis, the α-$f(\alpha)$ spectrum is the most widely used, and the most valid method to calculate the α-$f(\alpha)$ spectrum is wavelet-based singularity spectrum calculation[16]. The strength of singularity of function f at point x_0 can be given by the Hölder exponent $\alpha(x_0)$, the largest exponent where there exists a polynomial $P_n(x - x_0)$ of order $n < \alpha(x_0)$ and a constant $C > 0$, so that for any point x in a neighborhood of x_0, we have

$$\left|f(x) - P_n(x - x_0)\right| \le C\left|x - x_0\right|^{\alpha} \tag{3}$$

then $\alpha(x_0)$ is called the Hölder exponent of function f at point x_0. Therefore, the Hölder exponent can measure the nearness of the function to the polynomial. When the exponent is larger than one, the function is smooth, and the greater the exponent is, the nearer the function is to the polynomial. When the exponent is less than one, the function is irregular, and the lesser the exponent is, the farther the function is from the polynomial. To a remote sensing image, the Hölder exponent can respond to the obedience degree of the texture to some patterns, which is determined by the transform function used in decomposing the image; the larger the exponent, the higher the obedience.

To describe the singularity of all points or pixels of an image, we use the α-$f(\alpha)$ spectrum. The α-$f(\alpha)$ spectrum can describe the complex fractal body by classifying the body into sets of different singularities (α) and estimate the fractal dimension for each set. To get the α-$f(\alpha)$ curve of an image, three steps are necessary[17–20]: (1) calculate the Hölder exponent α for each pixel, (2) discover sets of pixels with the same α, (3) estimate the fractal dimension for each set of different α. For remote sensing image of rocks, the α-$f(\alpha)$ spectrum can not only measure the local irregularity of the

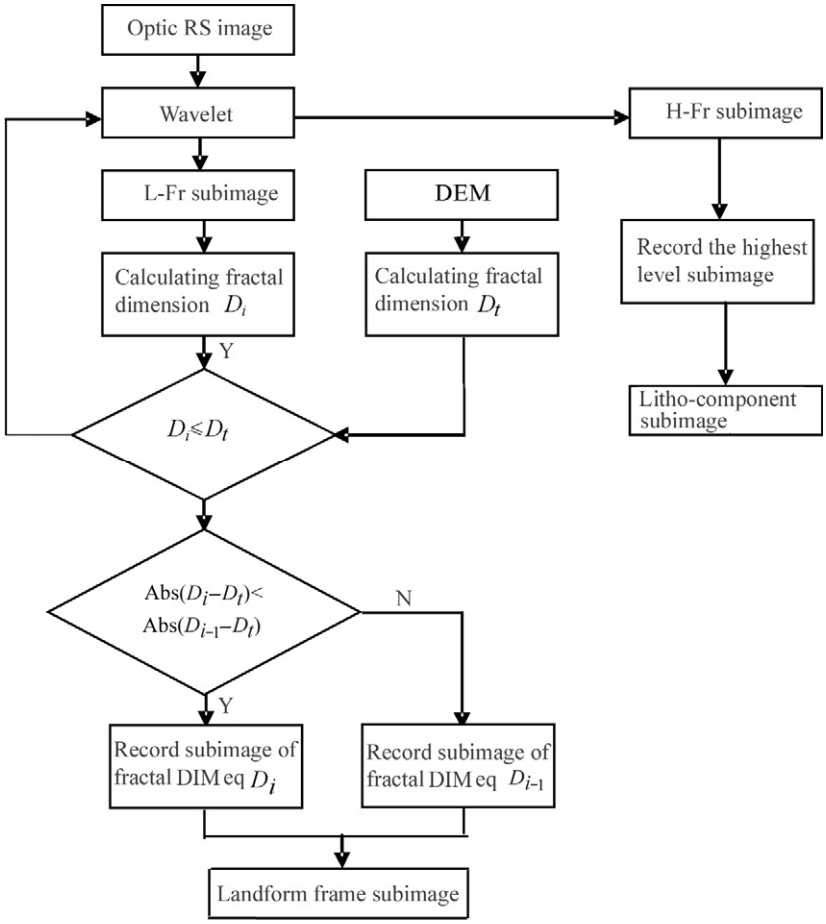

Fig. 1 Algorithm for decomposing RS image to landform frame and lithologic components

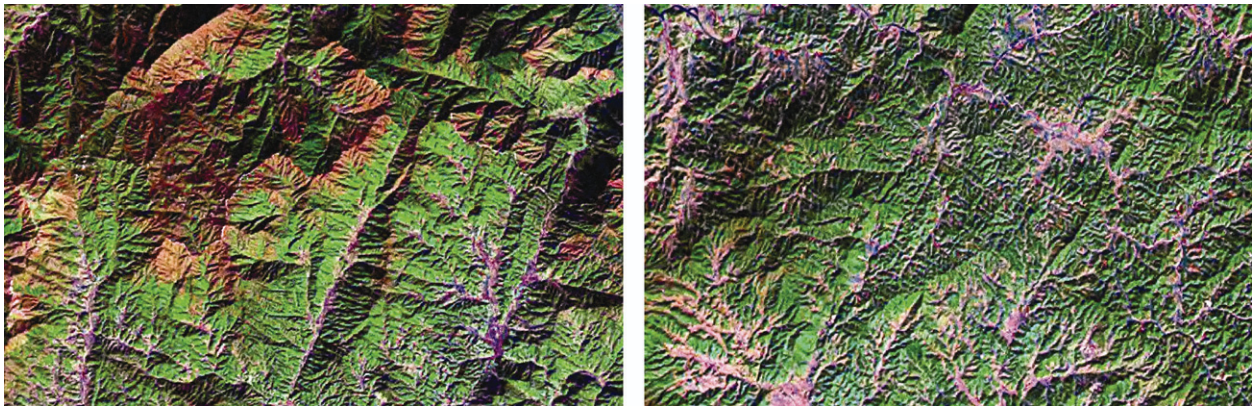

Fig. 2 ETM images of Miaoershan (left) and Xuehuading (right) adamellite plutons

river and gully and fracture and lithologic boundary, but also the complexity of these irregular sets in the whole image.

4.1 Multifractal feature of the ETM image of adamellite in different areas

In order to validate the decomposing algorithm for rock classification and identification by way of texture analysis with multifractal spectrum, ETM images of adamellite in Miaoershan of Guangxi and Xuehuading in Hunan were chosen. Visually, they were quite different in color, texture type, and density (Fig. 2), it was nearly impossible to judge them as identical rock types by visual interpretation.

On the raw ETM image, their multifractal spectra are quite different (Fig. 3). The α-$f(\alpha)$ spectra of Adamellite in Miaoershan spread in the Hölder exponent range from −0.43 to 0.55, and the plotted curve is asymmetrical on the two

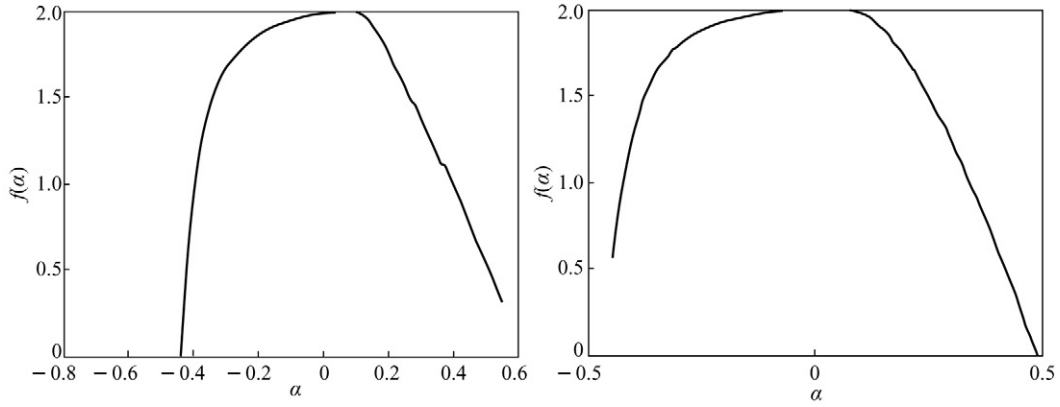

Fig. 3 α-$f(\alpha)$ spectra of ETM images of Miaoershan (left) and Xuehuading (right) plutons

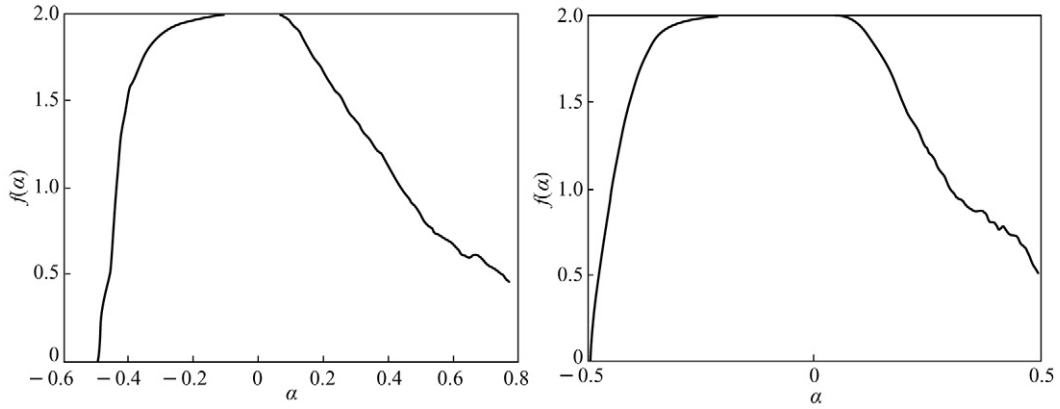

Fig. 4 α-$f(\alpha)$ spectra of landform frame subimages of Miaoershan (left) and Xuehuading (right) plutons

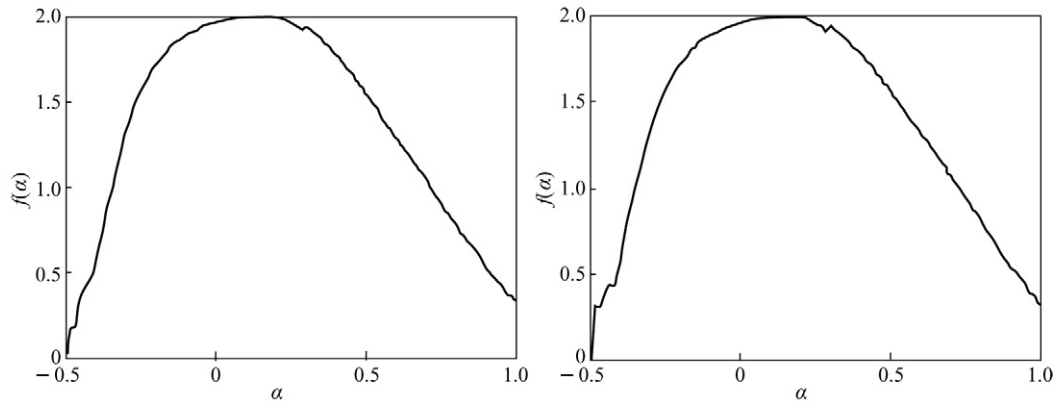

Fig. 5 α-$f(\alpha)$ spectra of horizontal lithologic component subimages of Miaoershan (left) and Xuehuading (right) adamellite

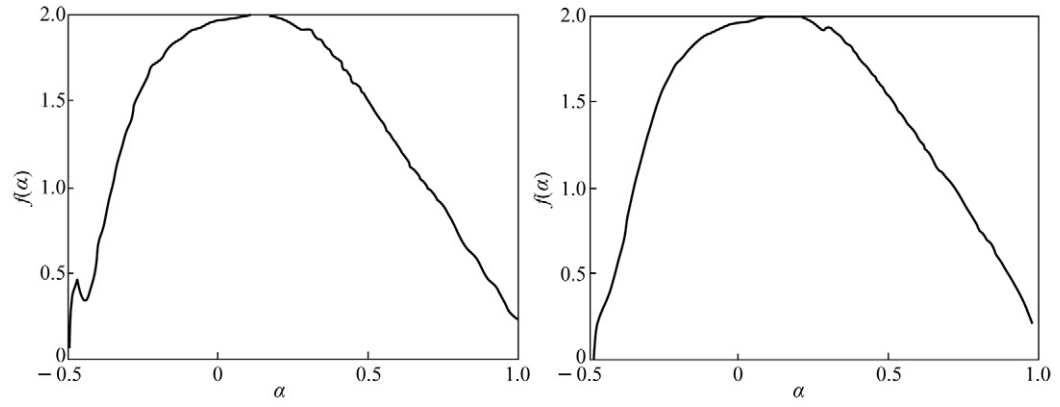

Fig. 6 α-$f(\alpha)$ spectra of the lithologic component subimages in diagonal direction of Miaoershan (left) and Xuehuading (right) adamellite

sides. On the side of the Hölder exponent less than 0, the shape is bell-like, indicating a certain continuity and self-similarity in the variation of the image texture. While on the side of the Hölder exponent greater than 0, the shape is a straight line, indicating that the fractal spectra are in linear distribution and are locally discontinuous, which implies that the image texture is more or less irregular in the macroscopic framework and the variations in texture are prominent, but with lower self-similarity.

In contrast to Miaoershan, the α-$f(\alpha)$ spectra of Adamellite in Xuehuading have two different features. First, the spectra spread in the Hölder exponent range from −0.5 to 0.5 is with better symmetry. Second, taking the 0-exponent as a boundary, the image can be divided into two parts. The part with exponent smaller than 0 has a wider distribution range, with high spectrum values, indicating that the variation of the fractal dimension is smooth and with higher self-similarity. While in the part with the exponent ≥0, the variation of fractal spectra is also smooth, but the variation of fractal dimension is continuous, indicating that the image texture is megascopically more regular, with higher self-similarity. Therefore, the multifractal of the raw ETM image does not show any lithologic relation or similarity between the two adamellites in the two areas.

Now let us examine the decomposed image; Figure 4 shows the α-$f(\alpha)$ spectrum of the landform frame subimages of the two areas, they are similar in shape, but different in the Hölder exponent range, one ranges from −0.5 to 0.8 and the other is between −0.5 and 0.5. This means the topographic frame of the two areas is different on the whole, but bears some similarities in local structure. Figure 5 is the α-$f(\alpha)$ spectrum of the lithologic component subimage of the two areas, in horizontal direction, they are nearly the same in shape and Hölder exponent range, the only slight difference is in the shape, which has occurred at the least Hölder exponent part. The α-$f(\alpha)$ spectrum of the lithologic component subimage in the diagonal direction also shows the same feature (Fig. 6), but the shape difference at the least Hölder exponent part is a slightly greater than that of the lithologic component image in the horizontal direction.

The different α-$f(\alpha)$ spectrum feature of the raw ETM image and the same α-$f(\alpha)$ spectrum feature of the lithologic component subimage of ETM image of adamellite in the two distant areas not only validates the effect of the image decomposed model and the algorithm, but also shows the possibility of classifying and identifying rock types, with image texture analysis by multifractal analysis.

4.2 Multifractal feature of ETM image of different rocks in the same area

In order to further validate the effect of the image decomposing algorithm, ETM images of Ordovician metamorphic sedimentary rocks are chosen for comparison with that of the adjacent adamellite. Visually, they look similar in texture frame with a dominant coarse texture which splits the image into two large terrains (Fig. 7). Furthermore there are some similarities between these terrains. This similarity is not exactly shown by the α-$f(\alpha)$ spectrum of raw ETM image (Fig. 8). Although the spectra are similar in Hölder exponent span, there are differences in the shape, especially on the side of the exponent larger than 0, The spectra of the metasedimentary rocks are convex, while that of the adamellite are concave. In addition there are differences at the zenith exponent (where the max $f(\alpha)$ occurs). The spectra zenith of metasedimentary rocks appears near exponent 0.1, while that of the adamellite appears near exponent 0. Therefore, the α-$f(\alpha)$ spectrum of the ETM image cannot indicate the similarity of the terrains.

However, the landform frame subimage decomposed by our algorithm can give a very similar α-$f(\alpha)$ spectrum (Fig. 9). The two spectra are similar in the Hölder exponent range, zenith exponent, and the total curve shape. The slight difference occurs only at the ends of the spectrum. The spectrum of the landform frame subimage of the metasedimentary rock vibrates at the smallest exponent, while the spectrum of the landform frame image of adamellite trembles at the largest exponent.

As the decomposed landform subimage of the two kinds of

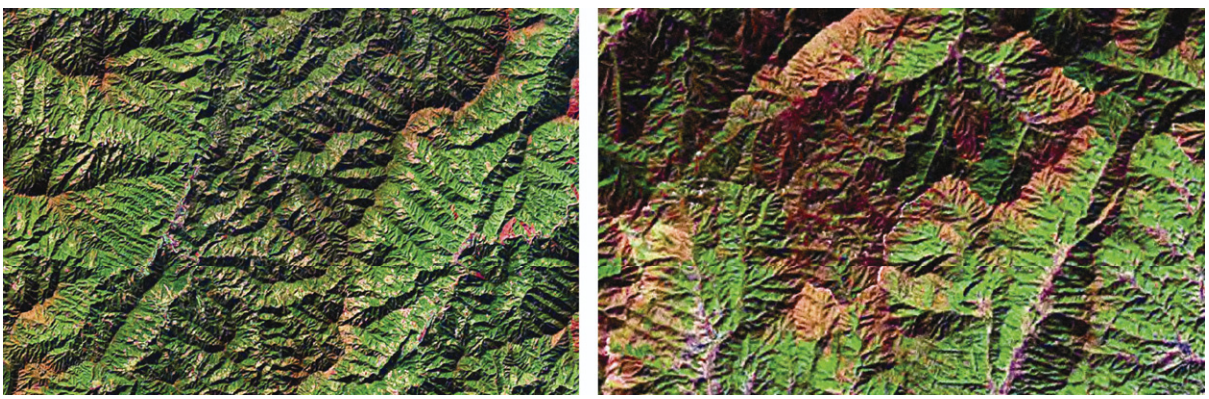

Fig. 7 ETM images of metasedimentary rocks (left) and adamellite plutons (right)

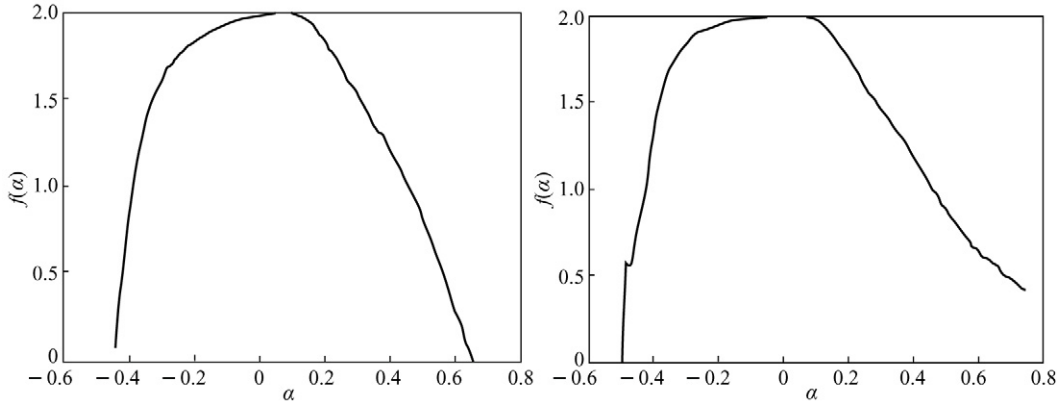

Fig. 8 α-$f(\alpha)$ spectra of ETM image of the metamorphic rock (left) and adamellite (right)

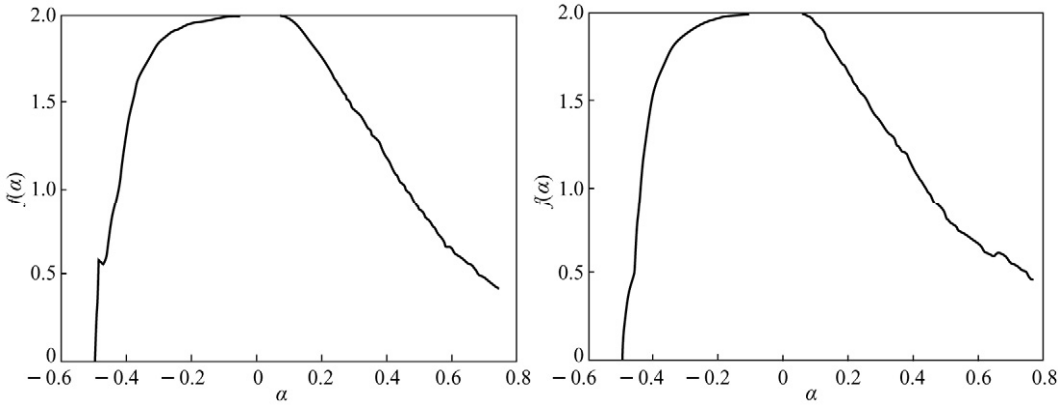

Fig. 9 α-$f(\alpha)$ spectra of the landform frame image of metasedimentary rock (left) and adamellite (right)

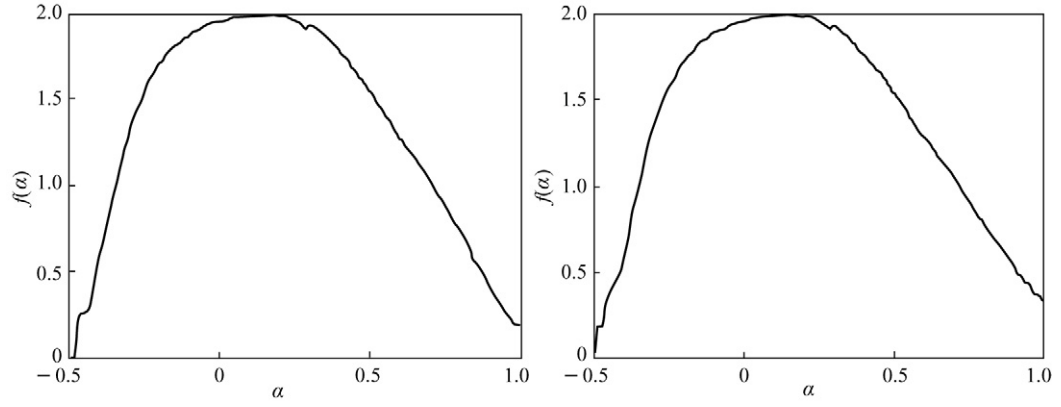

Fig. 10 α-$f(\alpha)$ spectra of horizontal component image of metasedimentary rock (left) and adamellite (right)

rocks bear the same α-$f(\alpha)$ spectrum, the multifractal difference of the raw ETM image must come from the lithologic component subimage. In the α-$f(\alpha)$ spectra of the horizontal lithologic component subimage of the two rocks, there is not much difference. On the contrary, they show more similarities than differences (Fig. 10). The Hölder exponent range, zenith exponent, and shape of the curve are nearly the same; the difference occurs on the largest exponent side where the spectrum for the metasedimentary rock is a little steeper than that for the adamellite. This means that the two rocks have nearly the same texture feature in horizontal direction. However, the α-$f(\alpha)$ spectra of the lithologic component subimage in diagonal direction of the two rocks are quite different (Fig. 11) in shape and exponent range. The spectra of the diagonal subimage of the metasedimentary rocks look like an asymmetrical or an incomplete bell and spread in the Hölder exponent range from −0.5 to 0.7, while that of the adamellite is a nearly symmetrical full bell and the exponent

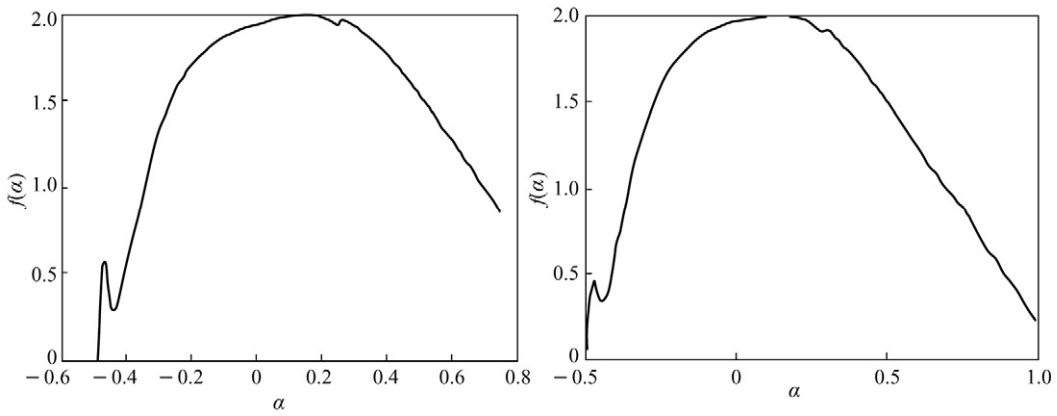

Fig. 11 α-$f(\alpha)$ spectra of diagonal component image of the metamorphic sandstone (left) and adamellite (right)

spreads from −0.5 to 1.0. The smaller Hölder exponent range of the lithologic component subimage in diagonal direction of the metasedimentary rock indicates that its texture is less regular or smooth than that of adamellite in diagonal direction, and this is correspondent to the visual effects. The inconsistent result of the lithologic component α-$f(\alpha)$ in different directions may come from the difference of anisotropy between the metasedimentary rock and adamellite. Anyway, the similar α-$f(\alpha)$ spectrum of the landform frame subimage of two neighboring rocks has validated the effect of our decomposing model and algorithm for remote sensing image.

5 Conclusions

Through the α-$f(\alpha)$ spectra study of ETM image and decomposed ETM image of adamellite and metasedimentary rocks, we have found the following facts: (1) the α-$f(\alpha)$ spectra of the raw ETM image do not show any clear relation to rock types or areal topography; (2) decomposed images of adamellite in different areas, by our algorithm, have the same α-$f(\alpha)$ spectra features of lithologic component subimage, but different α-$f(\alpha)$ spectra features of landform frame subimage; (3) decomposed metasedimentary rock and adamellite ETM images in the neighboring area by our algorithm bear similar α-$f(\alpha)$ spectra features of the landform frame subimage, but different spectra features of the lithologic component subimage in diagonal direction. Therefore, we have come to two conclusions: (1) our algorithm is validated to decompose remote sensing image into the landform frame subimage and lithologic component subimage; (2) multifractal spectra can be used to identify lithology in RS image only after understanding the geological meaning of the texture.

There are some questions that need to be discussed further for the multifractal study of rocks with remote sensing image. (1) Quantitive relation should be discussed between the α-$f(\alpha)$ spectra parameters and rock type; (2) The effects of wavelet base to image decomposition, the size of statistic windows to fractal dimention and spectrum are also need to study for the calculation precision.

References

[1] Pentland A. Fractal based description of natural scenes. *IEEE Transactions on Pattern Analysis and Machine Intelligence*, 1984, 9: 661–674.

[2] Jiang P, Shi S M. FBm texture analysis model and its application in rock recognition. *Journal of Remote Sensing*, 1995, 10(1): 38–43.

[3] Xue C S, Wang X. Methodology and application of remote sensing image texture analysis based on fractal geometry. *Geological Science and Technology Information*, 1997, 16(Suppl.): 99–105.

[4] Zhao J H, Yang S F, Chen H L. Recognition of lithology with remote sensing image based on fractal texture. *Remote Sensing Information*, 2004 (2): 2–4.

[5] Han S X, Qi D W, Yu L. Analysis and processing of decayed log CT image based on multifractal spectrum. *Forest Engineering*, 2007, 23(5): 15–18.

[6] Li P, Hu K L, Zhang B H. Design and application about computer program of material multifractal spectrum. *Journal of Nanjing University of Aeronautics and Astronautics*, 2004, 26(1): 78–81.

[7] Jia L, Wang T T. Computer modelling of the multifractal of fracture net work. *Journal of Geological Hazards and Environment Preservation*, 1997, 8(3): 48–53.

[8] Agterberg F P. Multifractal simulation of geochemical map patterns. *Earth Science*, 2001, 26(2): 142–151.

[9] Cheng Q M. Singularity of mineralization and multifractal distribution of mineral deposits. *Bulletin of Mineralogy, Petrology and Geochemistry*, 2008, 27(3): 298–305.

[10] Lu C S, Chung P C, Chen C F. Unsupervised texture segmentation via wavelet transform. *Pattern Recognition*, 1997, 30(5): 729–742.

[11] Laine A, Fan J. Texture classification by wavelet packet signature. *IEEE Transactions on Pattern Recognition and Machine Intelligence*, 1993, 15(11): 1186–1191.

[12] Zhu C Q, Yang X M. Study of remote sensing image texture

analysis and classification using wavelet. *International Journal of Remote Sensing*, 1998, 19(16): 3197–3203.

[13] Zhu X L, Peng F Y. Landform analysing method based on frame fractal dimension. *Infrared and Laser Engineering*, 2003, 32(5): 502–504.

[14] Zhang J X, Liu J. New method to establish mathematic model for landform. *Signal Processing*, 1997, 13(4): 369–373.

[15] Ao L B. Multifractal and description. *Modern Geophysic Knowledge*, 1996, 8 (Suppl.): 50.

[16] Soe W M, Nina S N L, John M T. Wavelets for urban spatial feature discrimination: Comparisons with fractal, spatial autocorrelation and spatial co-occurrence approaches. *Photogrammetric Engineering and Remote Sensing*, 2004, 70(7): 803–812.

[17] Arneodo A, Audit B, Kestener P, et al. Wavelet-based multifractal analysis. *Scholarpedia*, 2008, 3(3): 4103.

[18] Wen Y Z. Mathematic Foundation for Fractal Geometry. Shanghai: Shanghai Science and Education Publishing House, 2000.

[19] Lévy Véhel J. Introduction to the multifractal analysis of images. In: Fisher Y (ed.) Fractal Image Encoding and Analysis. Berlin: Springer Verlag, 1997.

[20] Lévy Véhel J, Legrand P. Signal and image processing with FRACLAB. In: Novak M M (ed.), Thinking in Patterns, Fractals and Related Phenomena in Nature. Singapore, London, New Jersey, Hong Kong: World Scientific Publishing Co., 2004.